

Extreme carrier shocking of intense long-wavelength pulses

Patrick Whalen,^{1,2} Paris Panagiotopoulos,^{2,3,*} Miroslav Kolesik,^{2,3,4} and Jerome V. Moloney^{1,2,3}

¹*Department of Mathematics, University of Arizona, Tucson 85721-0094*

²*Arizona Center for Mathematical Sciences, University of Arizona, Tucson 85721-0094*

³*College of Optical Sciences, University of Arizona, Tucson 85721-0094*

⁴*Constantine the Philosopher University, Nitra, Slovakia*

(Received 7 October 2013; published 28 February 2014)

We predict a paradigm shift in the nonlinear physics associated with ultrashort long-wavelength pulse propagation in gaseous and condensed media. Optical carrier shock formation, which profoundly modifies the underlying optical wave form, emerges prior to the onset of the well-known self-focusing collapse singularity. The canonical description of pulse propagation in this regime, where all nonlinear envelope descriptions fail, is identified as the full field carrier resolved modified Kadomtsev-Petviashvili (MKP) equation.

DOI: [10.1103/PhysRevA.89.023850](https://doi.org/10.1103/PhysRevA.89.023850)

PACS number(s): 42.65.Re, 42.65.Sf

The interaction of atoms and molecules with an intense ultrashort laser pulse plays a decisive role in a wide range of modern physics including higher-order harmonic generation, pulse propagation, and filamentation in gases. While much of the theory and experimental focus has been on near infrared pulse propagation [1,2], new exciting phenomena have recently been identified at longer mid-infrared wavelengths. In high pressure capillaries, the long interaction length in concert with filamentation of mid-IR pulses at 4 μm has been shown to generate bright coherent keV x-rays [3]. As the bandwidth of higher-order harmonic x-ray emission driven by mid-IR is enormous, spanning keV bandwidths, this should be sufficient to support few-cycle attosecond pulses. Very recently, the possibility of zeptosecond pulse generation at even longer wavelength pulses has been highlighted [4]. Access to these extreme bandwidths and very high harmonics will ultimately rely on propagation effects and precise control of longer wavelength pulses. In particular, the prediction of zeptosecond wave-form generation reported in Ref. [4] will need to be reassessed given that propagation effects need to be taken into account in light of the results presented here. Further significant progress in this emerging field of nonlinear physics will have to await the development of new pulsed few mJ laser sources at wavelengths beyond the 4 μm reported in Ref. [3].

To date, much of the nonlinear evolution of near-IR pulses can be qualitatively modeled with envelope models, which are generalizations of the nonlinear Schrödinger equation (NLSE), the best known being the nonlinear envelope equation (NEE) [1]. These mathematical models belong to a universal class of weakly nonlinear dispersive systems. While most past and recent experiments have been limited to the visible and near-infrared, these models provided an appropriate framework for intense pulse propagation. However, at longer mid-IR wavelengths the physics of the situation changes and the relative strength of nonlinearity and dispersion are interchanged. Moreover, the threshold for ionization rapidly increases, making it more difficult to generate free electrons. We shall see that these features profoundly change the nature of pulse propagation over extended path lengths. Rather than the blow-up self-focusing singularity dominating, we predict

that the underlying optical carrier wave exhibits extreme shock formation, as in the case of an ideal nondispersive medium [5].

In this article, we show that the canonical description of long-wavelength pulse propagation is the modified Kadomtsev-Petviashvili equation (MKP). It is closely related to the equation derived in the early 1980s by Kuznetsov for acoustic waves [6], for which equation with cubic nonlinearity various “blow up” results were found by Turitsyn and Fal’kovich [7], and more recently numerically studied in [8]. This model was first introduced in an optics setting by Kozlov *et al.* [9] who limited the discussion to one-dimensional (1D) solitary waves associated with few-cycle pulses and, subsequently, by Balakin [10] who investigated its mathematical properties relating to blow-up and shock singularity formation. In contrast to the NLSE and its many variants, this model is a full electromagnetic field resolved propagator. It can be systematically derived as an asymptotic expansion of the full vector Maxwell equations [10] or the unidirectional pulse propagation equation (UPPE) [11], in the limit of strong nonlinearity and weak dispersion. This stands in contrast to the NLSE which is the canonical description of weakly nonlinear, strongly dispersive behavior. Physically speaking, at long wavelengths, the material dispersion landscape becomes flat and featureless for most gases and many condensed materials and, consequently, we expect MKP to apply.

For illustrative purposes, we will present results on the nonlinear propagation of short-wavelength IR (SW-IR at $\lambda_0 = 2 \mu\text{m}$), mid-IR ($\lambda_0 = 4 \mu\text{m}$), and long-wavelength IR (LW-IR at $\lambda_0 = 8 \mu\text{m}$) pulses in xenon gas, and demonstrate with other medium models that the scenario we put forward is indeed universal. We show that optical carrier shocks dominate over the more traditional blow-up scenario typically associated with NLSE and NEE, and that rather exotic wave forms can be generated. The mechanism is akin to optical wave-form synthesis [12], with the crucial difference being that the process here is *spontaneous*. Importantly, shock formation occurs for both ultrashort and longer pulses although the latter case may lead to optical damage.

If $E(x, y, z, \tau = t - z/v_g)$ represents the dominant component of the electric field, then the MKP equation in nondimensional form is

$$\frac{\partial}{\partial \tau} \left(\frac{\partial E}{\partial z} + \frac{8L_0}{L_{NL}} E^2 \frac{\partial E}{\partial \tau} - \frac{L_0}{L_{DS}} \frac{\partial^3 E}{\partial \tau^3} \right) = \frac{L_0}{L_{DF}} \nabla^2 E. \quad (1)$$

*parisps@email.arizona.edu

Equation (1) shows how the right-going Riemann invariant E of the underlying wave equation is deformed over long distances by a combination of nonlinear, diffraction, and dispersion influences.

In Eq. (1), L_{NL} , L_{DS} , and L_{DF} correspond to the characteristic lengths for the nonlinear Kerr effect, dispersion, and diffraction, which are defined by

$$L_{NL} = \frac{c}{n_2 I_0 \omega_R}, \quad L_{DS} = \frac{1}{4a\omega^3}, \quad L_{DF} = \frac{k_R w_0^2}{2}, \quad (2)$$

where n_2 is the nonlinear refractive index of the material, I_0 is the initial pulse peak intensity, ω_R is a central frequency, and w_0 is the initial beam width at $1/e^2$ radius. We define L_0 to be the shortest distance (usually L_{NL} or L_{DF}) over which E changes. The coefficient a describes how the real part of the linear susceptibility deviates from a constant value. The canonical form of the MKP equation is generated from Eq. (1) by choosing $L_0 = L_{DF}$ and rescaling E .

Unless stated otherwise, the numerical experiments were conducted in xenon gas at 1-atm pressure. The nonlinear refractive index due to the instantaneous Kerr response is $n_2 = 5.8 \times 10^{-19} \text{cm}^2/\text{W}$ [13], and the dispersive relation is taken from [14]. Ionization can safely be ignored in the mid-IR and LW-IR regimes (for instance, $\lambda_0 = 8 \mu\text{m}$) since the combination of low energy photons (0.155 eV) and the relatively high ionization potential of xenon ($U_i = 12.03 \text{eV}$) would require extremely high light intensities to produce a significant plasma density. In addition, simulations performed with artificially increased ionization coefficients showed that a carrier wave shock will still manifest regardless of plasma generation and nonlinear losses (data not shown).

The input laser beam has a Gaussian spatiotemporal profile and is launched in xenon with an initial beam waist of 2 mm without any initial curvature. The central wavelength is $\lambda_0 = 8 \mu\text{m}$ and the pulse duration is 40 fs. The initial peak intensity is $I_0 = 1 \times 10^{13} \text{W/cm}^2$, which corresponds to approximately $3.79 P_{cr}$ in xenon, where $P_{cr} = 3.77 \lambda_0^2 / (8\pi n_0 n_2)$ is the critical power for self-focusing calculated for Gaussian beams. In order to explore a wide range of parameters, two additional wavelengths were used: $\lambda_0 = 4 \mu\text{m}$, and $2 \mu\text{m}$. The pulse duration and starting peak intensity are adjusted appropriately in order to keep the nonlinear length scale L_{NL} constant for all three cases. All simulations are done in radial geometry, time, and propagation distance, being essentially three-dimensional.

Figure 1 shows the electric field of the 8- μm pulse before and after the propagation of 5.63 cm inside xenon. We

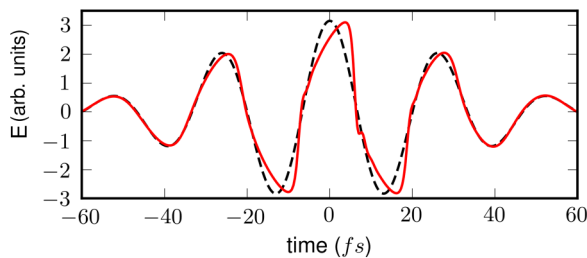


FIG. 1. (Color online) Electric field of an 8- μm , 40-fs laser pulse (black dashed line) undergoing self-steepening after 5.63-cm propagation in xenon gas (red continuous line).

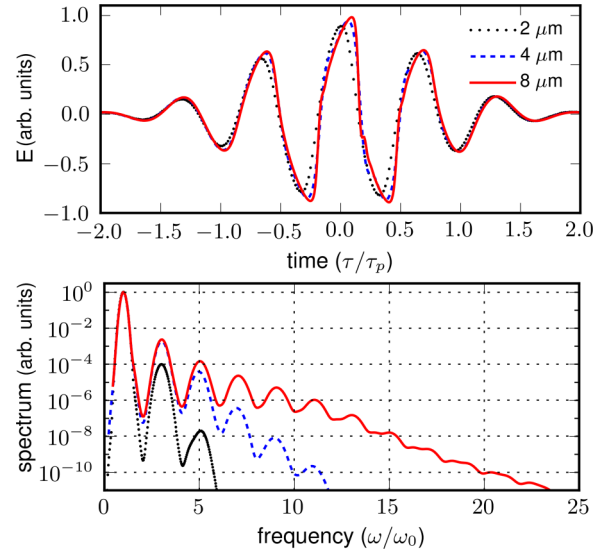


FIG. 2. (Color online) (a) Electric fields (at optimal distance), and (b) corresponding spectral intensities of three laser pulses after propagation in xenon gas. Black dotted line, $\lambda_0 = 2 \mu\text{m}$; blue dashed line, $\lambda_0 = 4 \mu\text{m}$; red continuous line, $\lambda_0 = 8 \mu\text{m}$. Horizontal axes are normalized to pulse duration τ_p and fundamental frequency ω_0 , respectively.

can clearly see that the electric field of the carrier wave is undergoing self-steepening, reforming into a smooth “shark-fin”-like shape. It is evident that the steepening of the electric field is proportional to its amplitude, since the center cycle is affected the most. Unlike other studies that have shown carrier shock formation in dispersionless media, this shock formation is predicted for a realistic dispersive medium.

In Fig. 2(a) we can see the dependence of the carrier shock on the initial wavelength. The temporal axis is scaled by the respective pulse durations (τ_p) so that the electric fields can be compared directly. As the wavelength is increased from $2 \mu\text{m}$, to $4 \mu\text{m}$, and finally $8 \mu\text{m}$, we can see that the optical shock becomes significantly more pronounced.

This behavior is reflected in the spectral domain, which is shown in Fig. 2(b). As before, the horizontal axis, here frequency, is scaled by the fundamental frequency ω_0 for each pulse, respectively. We can see that as the wavelength increases the number of generated harmonics and their amplitudes increase dramatically. In the case of the 8- μm beam, up to 10 odd harmonics are generated.

We identify this higher harmonic generation process as the driving force for carrier wave shock formation. The interaction of the generated higher harmonics with the fundamental carrier wave has the potential to generate a field shock. However, in order for the field shock to manifest itself and be observable, the different harmonics must co-propagate with the fundamental over a minimum distance, which can only be possible in weakly dispersive materials. The increase in field shock at longer wavelengths is therefore expected, since more harmonics reside in the flat dispersion regime and are able to co-propagate with the fundamental over a longer distance.

Note that although the electric field profiles for the 4- μm and 8- μm beams are almost identical, their respective spectral intensities differ significantly in amplitude after the third

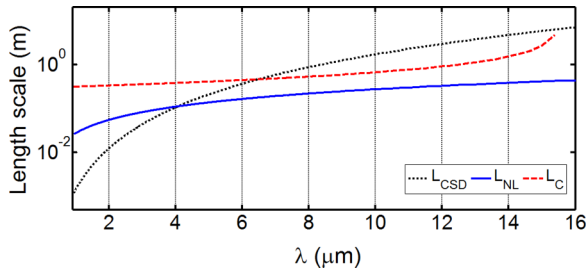


FIG. 3. (Color online) Characteristic lengths of various physical effects for xenon as a function of wavelength for an input intensity of $I_0 = 1 \times 10^{13}$ W/cm². Black dotted line, carrier shock dispersion length L_{CSD} ; blue continuous line, nonlinear length scale L_{NL} ; red dashed line, collapse distance L_C .

harmonic. From this observation we can infer that most of the steepening originates from the interaction between the third harmonic and fundamental, since the additional higher harmonics have only a small impact on the field shape. Additional simulations showed that when the spectrum is artificially truncated after the third harmonic, most of the steepening seen in the full spectral box case is preserved (data not shown).

Motivated by this observation, we introduce a new characteristic length, describing the carrier wave shock dispersion defined as

$$L_{\text{CSD}} = \frac{1}{\omega_0^2 |k''(3\omega_0) - k''(\omega_0)|}. \quad (3)$$

L_{CSD} is effectively a way to measure how fast the fundamental and the third harmonic will walk off, dispersing the effect of self-steepening on the carrier wave. Note the shock dispersion does in fact not depend on the pulse duration of the wave packet, which means that carrier shock formation is expected for a wide range of pulse durations given sufficiently high peak intensity.

We can now compare the importance of the relevant physical effects with respect to their characteristic lengths, namely the carrier shock dispersion L_{CSD} , the nonlinear length L_{NL} , and the collapse distance L_C defined in [15]. In Fig. 3 we can see the characteristic lengths plotted as a function of wavelength for an input peak intensity of $I_0 = 1 \times 10^{13}$ W/cm². Note that at a given wavelength the effect with the shortest length scale is the one defining the propagation. As we can clearly see, at near-IR up to 4 μm , dispersion is dominant, which means that a carrier shock is unlikely to occur. Since power is above the critical value, beam collapse will occur at the distance estimated by the red dashed line. This prediction is in agreement with the extensive literature found for the classical femtosecond filamentation regime for near-IR and SW-IR (700 nm–3 μm) pulses [1,2].

However, at 4 μm the blue and black lines cross, which means that a transition from the blowup to the carrier wave shock scenario is taking place. After 4 μm the nonlinear length scale is the shortest of the three, and the field shock is predicted to appear first since the walk-off between the harmonics is not fast enough to suppress it. In this regime power is still above critical, however, the collapse distance is much longer than the nonlinear length scale and therefore a carrier wave shock should always be observed.

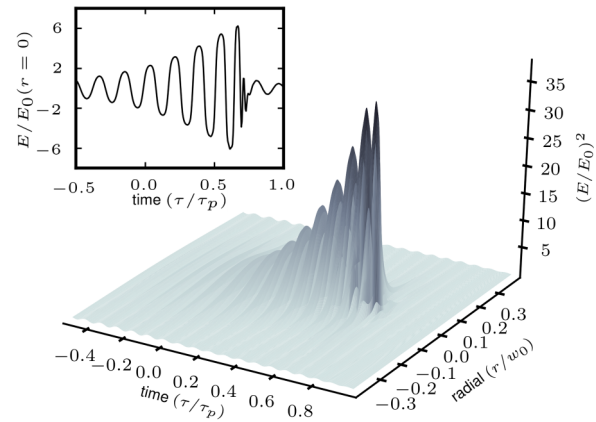


FIG. 4. Electric field of a $\lambda_0 = 2$ μm laser pulse undergoing critical collapse in xenon gas. The input power is $P = 3P_{cr}$ with a beam waist $w_0 = 2$ mm and pulse duration $\tau_p = 40$ fs. The spatiotemporal profile of the square of the electric field is shown at a propagation distance of $z = 66$ cm. The inset shows the on-axis field at the same propagation distance.

In the discussion so far, the shock development has been quasi-1D due to the much longer characteristic blow-up length scale L_C . Consequently radial points across the transverse beam remain essentially uncoupled as the shock develops. An interesting point to address is to see how these two classic singularities can conspire to accelerate or mediate shock formation in some manner. Referring to Fig. 3, we expect that if we are below the 4- μm intersection point of nonlinear length and shock dispersion scale, it may be possible that increasing peak intensity associated with the development of the collapse singularity will cause the effective nonlinear length to move below the shock dispersion length. If so, we would expect the blow-up to nucleate a carrier shock singularity as it develops. Figure 4 illustrates this strong spatiotemporal coupling at a point well along the classical collapse singularity curve where the intensity has increased tenfold. While the shock structure is evident in the 1D field slice (inset), it is somewhat smoothed by the walk-off of the third harmonic arising during the adiabatic intensity growth associated with self-focusing.

Of course an obvious way of accelerating carrier shock development in the absence of blow-up is to simply strongly focus the beam. The significantly increased intensity in the focal region forces the carrier shock to appear earlier. Figure 5 shows the effect the initial phase-front curvature of $f = 10$ cm has on the electric field shape after 7.33 cm of propagation in

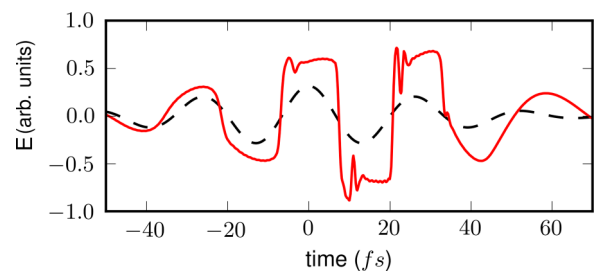


FIG. 5. (Color online) Effect of initial curvature of $f = 10$ cm on the carrier shock formation after propagation of 7.33 cm in xenon.

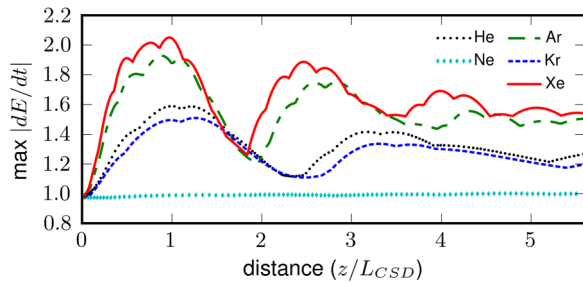


FIG. 6. (Color online) Carrier shock strength as a function of propagation distance normalized in shock dispersion lengths, for all five noble gases. In all cases the input pulse is 20-fs long, has a wavelength of $\lambda_0 = 4 \mu\text{m}$ and an initial peak intensity of $I_0 = 5 \times 10^{12} \text{ W/cm}^2$.

xenon. Focusing the beam clearly accelerates shock development leading to extreme wave forms that exhibit a radical departure from a sinusoidal shape. Now the electric field signal polarity switches extremely quickly within a fraction of the fundamental optical cycle. Similar field shapes were obtained recently in [12,16] through synthesis of appropriately modulated higher harmonics, for 3.5-ns pulses at low power. In our case, however, the wave packets are spontaneously generated in the medium, and carry over $3P_{cr}$ at 40-fs duration. This observation suggests a means of controlling optical carrier wave forms for future studies in extreme nonlinear optics.

We performed additional simulations for other noble gases with roughly the same input parameters, in order to verify that this propagation regime is indeed quite generic. The results can be seen in Fig. 6, where the maximum of the derivative of the field is plotted as a function of propagation

distance, normalized in terms of L_{CSD} so that the curves for the different gases can be directly compared. As we can see xenon is clearly the optimal medium of the five to observe carrier field shock. However, almost all other noble gases exhibit this behavior to some extent, with the exception of Neon. The difference in carrier shock strength can be explained with the analysis used in Fig. 3, since different materials have different dispersion curves [14] and nonlinearity. Thus even though the mechanisms leading to carrier shock formation are very generic, input beam characteristics have to be chosen properly and according to the medium.

To summarize, we have shown through numerical experiments that the MKP model can accurately predict carrier wave shock formation for mid-IR and LW-IR wavelengths in xenon gas, exhibiting a “shark-fin”-like electric field shape. The carrier wave self-steepening is explained as the interaction between the co-propagating higher harmonics with the fundamental. A comparison between the characteristic lengths for shock dispersion, nonlinearity, and beam collapse reveals the transition from the classical blowup scenario to carrier wave shock formation as we move from near-IR to longer wavelengths. In addition, controlling the carrier wave shock profile through focusing of the beam, can result in the generation of novel almost “top-hat” field profiles.

ACKNOWLEDGMENTS

We would like to thank Ewan Wright for the fruitful discussion and his help regarding material properties. This work was supported by an Air Force Office of Scientific Research Multidisciplinary University Research Initiative (MURI) Grant No. FA9550-10-1-0561.

-
- [1] A. Couairon and A. Mysyrowicz, *Phys. Rep.* **441**, 47 (2007).
 - [2] A. Couairon, E. Brambilla, T. Corti, D. Majus, O. d. J. Ramírez-Góngora, and M. Kolesik, *The European Physical Journal Special Topics* **199**, 5 (2011).
 - [3] T. Popmintchev, M.-C. Chen, D. Popmintchev, P. Arpin, S. Brown, S. Ališauskas, G. Andriukaitis, T. Balčiūnas, O. D. Mücke, A. Pugzlys *et al.*, *Science* **336**, 1287 (2012).
 - [4] C. Hernández-García, J. A. Pérez-Hernández, T. Popmintchev, M. M. Murnane, H. C. Kapteyn, A. Jaron-Becker, A. Becker, and L. Plaja, *Phys. Rev. Lett.* **111**, 033002 (2013).
 - [5] R. G. Flesch, A. Pushkarev, and J. V. Moloney, *Phys. Rev. Lett.* **76**, 2488 (1996).
 - [6] E. A. Kuznetsov, S. L. Musher, and A. V. Shafarenko, *JETP Lett.* **37**, 241 (1983).
 - [7] S. K. Turitsyn and G. E. Fai'kovich, *Zh. Eksp. Teor. Fiz.* **89**, 270 (1985).
 - [8] C. Klein and J.-C. Saut, *J. Nonlinear Sci.* **22**, 763 (2012).
 - [9] S. A. Kozlov and S. V. Sazonov, *J. Exp. Theor. Phys.* **84**, 221 (1997).
 - [10] A. A. Balakin, A. G. Litvak, V. A. Mironov, and S. A. Skobelev, *J. Exp. Theor. Phys.* **104**, 363 (2007).
 - [11] M. Kolesik and J. V. Moloney, *Phys. Rev. E* **70**, 036604 (2004).
 - [12] H.-S. Chan, Z.-M. Hsieh, W.-H. Liang, A. H. Kung, C.-K. Lee, C.-J. Lai, R.-P. Pan, and L.-H. Peng, *Science* **331**, 1165 (2011).
 - [13] J. K. Wahlstrand, Y.-H. Cheng, and H. M. Milchberg, *Phys. Rev. Lett.* **109**, 113904 (2012).
 - [14] A. Bideau-Mehu, Y. Guern, R. Abjean, and A. Johannin-Gilles, *J. Quant. Spectrosc. Radiat. Transfer* **25**, 395 (1981).
 - [15] J. H. Marburger, *Prog. Quantum Electron.* **4**, 35 (1975).
 - [16] S. N. Goda, M. Y. Shverdin, D. R. Walker, and S. E. Harris, *Opt. Lett.* **30**, 1222 (2005).